DOI: 10.1002/chem.200700616

Origin of Diastereoselectivity in the Organolanthanide-Mediated Intramolecular Hydroamination/Cyclisation of Aminodienes: A Computational Exploration of Constrained Geometry CGC–Ln Catalysts**

Sven Tobisch*[a]

Abstract: The regulation of ring-substituent diastereoselectivity in the intramolecular hydroamination/cyclisation (IHC) of α-substituted aminodienes by constrained geometry CGC–lanthanide catalysts (CGC = $[Me_2Si(\eta^5\text{-}Me_4C_5)(t\text{BuN})]^{2-}$) has been elucidated by means of a reliable DFT method. The first survey of relevant elementary steps for the 1-methyl-(4*E*,6)-heptadienylamine substrate (**1**) and the $[\{Me_2Si(\eta^5\text{-}Me_4C_5)(t\text{BuN})\}Sm\{N(TMS)_2\}]$ starting material (**2**) identified the following general mechanistic aspects of Ln-catalysed aminodiene IHC. The substrate-adduct **3**-S of the active CGC–Ln–amidodiene compound represents the catalyst's resting state, but the substrate-free form **3′** with a chelating amidodiene functionality is the direct precursor for cyclisation. This step proceeds with almost complete regioselectivity through exocyclic ring closure by means of a frontal trajectory, giving rise to the CGC–Ln–azacycle intermediate **4**. Subsequent protonolysis of **4** is turnover limiting, whilst the ring-substituent diastereoselectivity is dictated by exocyclic ring closure. Unfavourable close interatomic contacts between the substrate's α-substituent and the catalyst backbone have been shown to largely govern the *trans*/*cis* selectivity. Substituents of sufficient bulk in the α-position of the substrate have been identified as being vital for stereochemical induction. The present study has indicated that the diastereoselectivity of ring closure can be considerably modulated. The variation of the lanthanide's ionic radius and introduction of extra steric pressure at the substrate's α-position and/or the CGC N centre have been identified as effective handles for tuning the selectivity. The quantification of these factors reported herein represents the first step toward the rational design of improved CGC–Ln catalyst architectures and will thus aid this process.

Keywords: density functional calculations · diastereoselectivity · hydroamination · lanthanides · reaction mechanisms

Introduction

Hydroamination, namely the catalytic direct addition of an amine N–H bond across a carbon–carbon multiple bond, is a challenging and highly desirable transformation, which has provoked diverse research activities. The intramolecular hydroamination/cyclisation (IHC) of amine-tethered carbon–carbon unsaturated linkages is the most efficient, atom-economical and direct route toward functionalised nitrogen heterocycles.[1] This process is mediated by a variety of compounds from across the Periodic Table, with organolanthanide complexes[2] in particular being appealing.[3,4] The development of catalysts for the stereoselective formation of five- to seven-membered azacycles is of paramount interest to both academia and industry.[1] Various Ln–ligand architectures have been developed in recent years.[4] Noteworthy is the half-lanthanocene, $[(CGC)Ln\{E(TMS)_2\}]$ "constrained geometry" family of precatalysts (CGC = $[Me_2Si(\eta^5\text{-}Me_4C_5)(t\text{BuN})]^{2-}$),[5] $[\{Me_2Si(\eta^5\text{-}Me_4C_5)(t\text{BuN})\}Ln\{E(SiMe_3)_2\}]$ (E = N, CH). These coordinatively relatively open compounds exhibit significantly enhanced activity and are of particular value when dealing with sterically encumbered substrates, for which most conventional catalysts fail.[5b,6] The ability of CGC–Ln complexes to mediate the cyclohydroamination in a stereoselective fashion has been furthermore demonstrated for aminodienes and other substrate classes.[6,7]

Marks and co-workers proposed a generally accepted mechanistic scenario for organolanthanide-mediated IHC,[4b] which exhibits the following features common to the various

[a] Dr. S. Tobisch
University of St Andrews, School of Chemistry
Purdie Building, North Haugh, St Andrews
Fife KY16 9ST (UK)
Fax: (+44) 1707-383-652
E-mail: st40@st-andrews.ac.uk

[**] CGC = $[Me_2Si(\eta^5\text{-}Me_4C_5)(t\text{BuN})]^{2-}$.

Supporting information for this article is available on the WWW under http://www.chemeurj.org/ or from the author.

amine-tethered unsaturated carbon–carbon linkages: 1) smooth precatalyst activation through protonolytic cleavage of the Ln–E(TMS)$_2$ bond by the substrate, 2) an overall large negative activation entropy $\Delta S^{\ddagger}$ and 3) a reaction rate that is first order in [catalyst] and zero order in [amine substrate]. This mechanism has been confirmed and complemented by recent computational studies.[8,9] Scheme 1 shows a simplified catalytic cycle for the organolanthanide-mediated IHC of the α-substituted 1-methyl-(4*E*,6)-heptadienylamine substrate (**1**) in the presence of [(CGC)Ln{N(TMS)$_2$}] starting material **2**.[10] This scheme comprises exclusively of pathways for cyclisation and protonolysis, which are relevant for rationalising the regio- and stereoselectivity of cycloamine formation, as revealed from our previous computational mechanistic investigation, in which a more elaborate mechanism can be found.[8b] Firstly, precatalyst **2** is smoothly transformed into the amidodiene–Ln compound through protonolysis at the Ln–N(TMS)$_2$ bond by **1**. The catalytically active amidodiene–Ln complex can exist in substrate-free forms with a monohapto (**3**) or chelating (**3′**) amidodiene moiety, respectively, and also as substrate adduct **3**-S; all of which are likely to be readily interconvertable. Subsequently, the diene C=C linkage adds across the Ln–N functionality of **3′** to afford azacyclic intermediates. This step can proceed through regioisomeric *exo*- and *endo*-cyclic pathways. Intermediate **4**, bearing a 2,5-substituted five-membered azacycle tethered to an allylic functionality, is formed by 5-*exo* cyclisation, whilst the alternative 6-*endo* pathway leads to **5** with a vinylic α-side chain linked to a 2,6-substituted six-membered azacycle. Ensuing protonolysis of intermediates **4** and **5** by **1** yields first cycloamine–amido–Ln compounds, from which the cycloamine products are readily liberated to regenerate the catalytically active amidodiene–Ln complex and complete the cycle. 2-Methyl-6-vinyl-piperidine **P7** is generated by protonolysis of **5** along the 6-*endo* cyclisation initiated route. Of the various paths for protonation of the allylic tether of **4**, proton transfer onto the terminal C^8 centre is most accessible kinetically.[8b] This leads to the cycloamine–amido–Ln compound **6a**, and furthermore directly to 2-methyl-5-[(*E*)-prop-1-enyl]pyrrolidine (**P6a**), which is the predominantly generated cycloamine (see below).[11]

The coordinatively relative open CGC–Ln catalysts, when employed in aminodiene IHC, exhibit complete regioselectivity for ring closure, good to excellent ring-substituent diastereoselectivity and also good *E*-double-bond selectivity. The α-substituted 1-methyl-(4*E*,6)-heptadienylamine (**1**) together with [(CGC)Sm{N(TMS)$_2$}] precatalyst **2** yields exclusively pyrolidines **P6** with excellent stereocontrol for both 2,5-*trans* substitution (*trans*/*cis* 90:10) and *trans* geometry of the alkene tether (with **P6a** being the predominant product), whilst piperidines **P7** are not among the products (Scheme 2).[7]

Herein, we present the computational exploration of the experimentally studied IHC of **1** by precatalyst **2**,[7] which covers all relevant steps to afford the predominant product

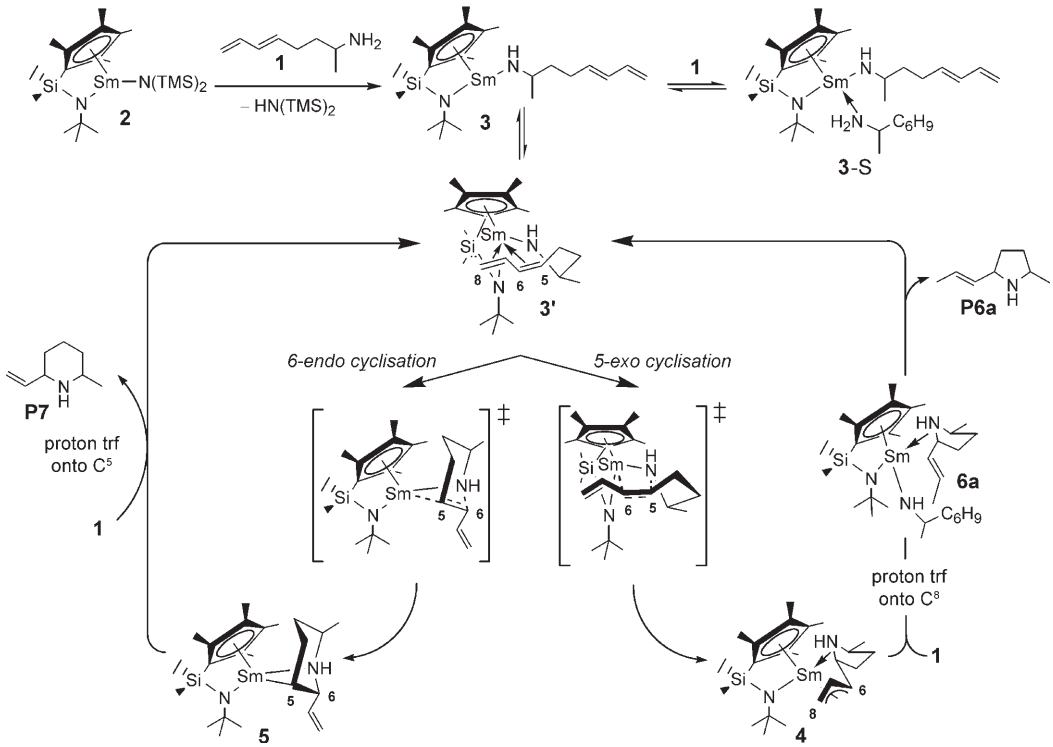

Scheme 1. Simplified catalytic reaction course for the organolanthanide-mediated intramolecular hydroamination/cyclisation of aminodienes to afford functionalised five- and six-membered azacycles, based on experimental studies of Marks and co-workers.[4b,7] For a more elaborate mechanism see reference [8b]. The 1-methyl-(4*E*,6)-heptadienylamine (**1**) and the [(CGC)Sm{N(SiMe$_3$)$_2$}] complex (**2**) were chosen as prototypical α-methyl-substituted substrate and CGC–Ln precatalyst, respectively.

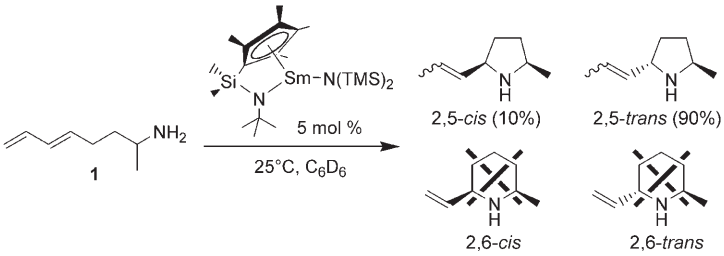

Scheme 2.

P6a (Scheme 1). The present study intends to elucidate what factors determine the observed high diastereoselectivity of the intramolecular C–N bond formation. Moreover, the sensitivity of the ring closure towards the size of the lanthanide ion and some steric pressure introduced at the CGC nitrogen centre is gauged computationally. As the rationalisation and quantification of these factors represents the first step toward the rational design of improved CGC–Ln catalysts architectures, the insights provided herein will assist this process.

This manuscript is organised as follows: First, the most accessible pathways of all relevant steps that give rise to the predominant cycloamine **P6a** will be explored. This will lead to the identification of which steps are the rate- and selectivity-determining steps and whether they coincide. Afterwards, the origin of the ring-substituent diastereoselectivity will be elucidated. A further section is devoted to the exploration of how the lanthanide-ion size and an increase in steric encumbrance at the catalyst backbone affect the stereoselective outcome.

Results and Discussion

Exploration of relevant elementary steps: In this first part of the study, the most favourable of the various stereochemical pathways for each of the relevant steps that lead to cycloamine **P6a** will be discussed.

Precatalyst activation: Effective catalysis entails the initial smooth transformation of the starting material **2** into the catalytically active amidodiene–Sm compound (Scheme 1). This process is structurally characterised in the Supporting Information (Figure S1), whilst the energetics are collected in Table 1. Protonolytic cleavage of the Sm–$N(TMS)_2$ bond by **1** proceeds first with formation of the encounter complex **2**-S, which is slightly downhill ($\Delta G = -1.3$ kcal mol^{-1}) and requires overcoming a free-energy barrier of 17.0 kcal mol^{-1} for subsequent proton transfer. The conversion of **2** into the amidodiene–Sm compound is slightly exergonic (Table 1), thereby indicating a clean and sufficiently facile transformation, as observed by NMR spectroscopy.[7] Species **3′**, which contains a chelating amidodiene moiety, is the thermodynamically most favourable of the substrate-free forms **3** and **3′** of the active amidodiene–Sm complex; both of which are readily interconvertible[25] and are in equilibrium (Table 1, Figure S1 in the Supporting Information). Complexation of an additional molecule **1** to **3**⇄**3′** is kinetically facile and downhill, leading to **3**-S with a η^1-amidodiene moiety as the most stable adduct species ($\Delta G = -5.0$ kcal mol^{-1} relative to {**3′**+**1**}, Figure S1 in the Supporting Information).

Intramolecular cyclisation: The thermodynamically favourable species **3′** of the substrate-free forms with a chelating amidodiene moiety is the direct precursor for the most accessible pathway for both the *endo* and *exo* cyclisation. Similar to the findings of our previous study,[8b] additional substrate molecules do not appear to assist this process.[26] Two different trajectories have already been proposed (Scheme 3);[27] firstly, the frontal approach of the C=C

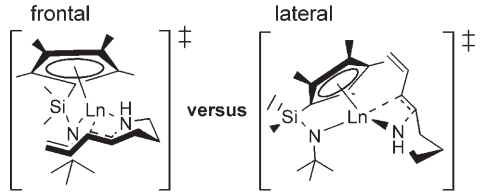

Scheme 3.

double bond along the ring-centroid–Ln–N bisector, and secondly, the lateral approach along the perpendicular of the ring-centroid–Ln–N plane. Ring closure is found to occur exclusively by the frontal approach, whilst the Cp ring and N*t*Bu group exert significant steric pressure on the inserting diene functionality along the lateral trajectory.

The two regioisomeric pathways exhibit distinctly different structural features, as shown in Figure 1. Formation of the five-membered azacyclic intermediate **4** proceeds through a chairlike transition state TS[**3′**–**4**] which constitutes C^5–N bond formation together with concomitant transformation of the *trans* diene moiety into a *syn*-η^3-butenyl functionality. Noteworthy, the diene's C^7=C^8 double bond, which does not participate in the ring closure, assists the process by stabilising the lanthanide centre coordinatively. Following the reaction path further leads directly to **4**, which has the azacycle coordinated by its N-donor centre and also by the *syn*-η^3-butenyl tether

Table 1. Energy profile for protonolysis of precatalyst **2** by aminodiene substrate **1**.[a,b]

Protonolysis pathway	Substrate encounter complex	TS	Products[c]
1+ **2**→**3**+$HN(TMS)_2$	−8.7/*−1.3* (**2**-S)	8.8/*17.0*	4.6/*4.1* (**3**) −1.8/*−1.4* (**3′**)

[a] Total barriers and reaction energies are relative to {**1**+**2**}. [b] Activation enthalpies and free energies ($\Delta H^{+}/\Delta G^{+}$) and reaction enthalpies and free energies ($\Delta H/\Delta G$) are given in kilocalories per mole; numbers in italic type are the Gibbs free energies. [c] See the text (or Figure 1) for a description of the various isomers of the amidodiene–Sm complex.

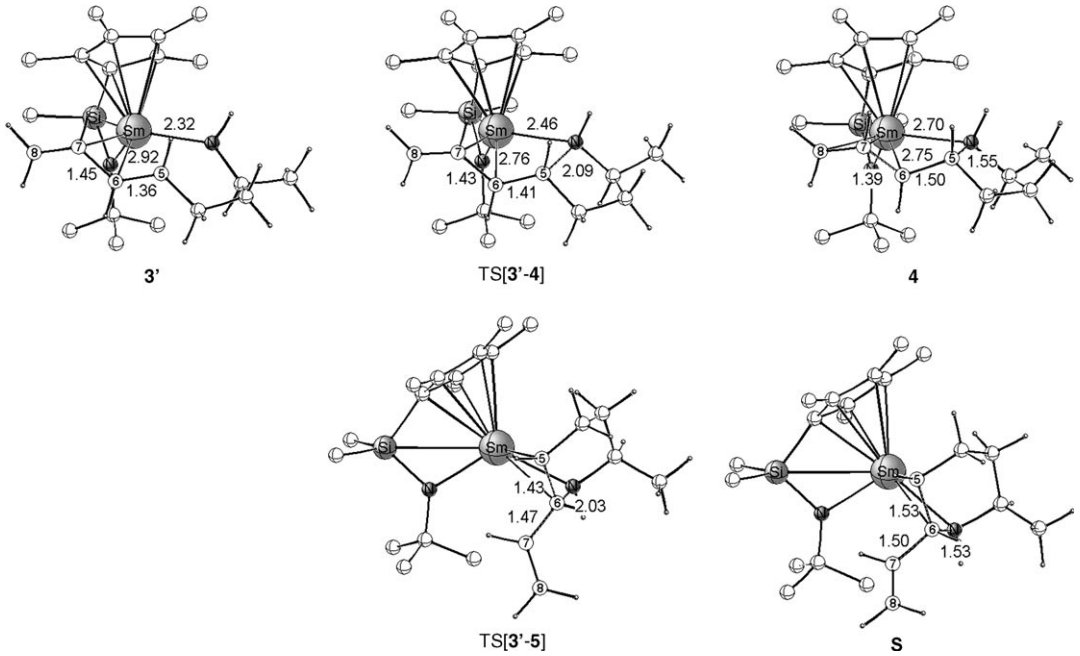

Figure 1. Selected structural parameters [Å] of the optimised structures of key species for 5-*exo* (*trans*-2,5 (*Re*) pathway, top) and 6-*endo* (*trans*-2,6 (*Re*) pathway, bottom) ring closure. The cut-off for drawing Sm–C bonds was arbitrarily set to 3.1 Å. The hydrogen atoms on the CGC backbone are omitted for the sake of clarity.

group to Sm (Figure 1). Isomers of **4** with a cleaved Sm–N bond and/or a η^1-butenyl–Sm ligation are found to be at higher energy. On the other hand, 6-*endo* cyclisation is seen to not benefit from a coordinative stabilisation of the Sm centre by the emerging vinyl tether group. Ring closure by C^6–N bond formation occurs through the productlike TS[**3′**–**5**], in which the vinyl group is almost completely preformed already. This leads to **5** with a η^2-azacycle–Sm ligation in the prevalent isomer, whilst the vinyl group does reside outside of the immediate proximity of the lanthanide centre.

These structural aspects are paralleled in the computed energy profiles. Exocyclic ring closure is facile with a moderate barrier of 5.5 kcal mol^{-1} ($\Delta G^{\neq}$) and driven by a small thermodynamic force ($\Delta G = -1.9$ kcal mol^{-1}, Table 2). In contrast, 6-*endo* cyclisation is predicted to be difficult kinetically, as it requires overcoming a substantial barrier of 31.8 kcal mol^{-1} ($\Delta G^{\neq}$), and is furthermore strongly endergonic ($\Delta G = 23.2$ kcal mol^{-1}, Table 2). Of the alternative pathways, exocyclic ring closure is clearly seen to be distinctly favourable, due to both kinetic ($\Delta\Delta G^{\neq} = 25.3$ kcal mol^{-1}) and thermodynamic ($\Delta\Delta G = 25.1$ kcal mol^{-1}) considerations. This strong preference has its primary origin in electronic factors, as only small reorganisations for **3′**→TS-[**3′**–**4**] are required and the second C^7=C^8 double bond assists the process coordinatively; it also matches the empirical rules by Baldwin.[28] Accordingly, ring closure proceeds with almost complete regioselectivity through **3′**→**4**, thereby rationalising that piperidines are not in the product spectrum.

Table 2. Energy profile for cyclisation through regioisomeric 5-*exo* and 6-*endo* pathways.[a,b]

Cyclisation pathway	Precursor[c]	TS	Product[d]
5-*exo*	6.5/*5.6* (**3**)		
2,5-*cis* (*Re*)	2.1/*2.3* (**3′**)	6.8/*8.2*	−2.1/*−0.3* (**4**)
2,5-*cis* (*Si*)	3.3/*3.5* (**3′**)	8.5/*10.1*	0.6/*2.6* (**4**)
2,5-*trans* (*Re*)	0.1/*0.1* (**3′**)	4.2/*5.5*	−3.7/*−1.9* (**4**)
2,5-*trans* (*Si*)	0.0/*0.0* (**3′**)	4.5/*5.8*	−2.9/*−1.2* (**4**)
6-*endo*[e]			
2,6-*cis* (*Re*)	2.1/*2.3* (**3′**)	30.0/*31.8*	21.2/*23.2* (**5**)
2,6-*trans* (*Re*)	0.1/*0.1* (**3′**)	34.9/*36.7*	23.5/*25.5* (**5**)

[a] Total barriers and reaction energies are relative to the favourable isomer **3′** of the substrate-free form of the amidodiene–Sm complex, which has a chelated amidodiene functionality. [b] Activation enthalpies and free energies ($\Delta H^{\neq}/\Delta G^{\neq}$) and reaction enthalpies and free energies ($\Delta H/\Delta G$) are given in kilocalories per mole; numbers in italic type are the Gibbs free energies. [c] See the text (or Scheme 1) for description of the various forms of the amidodiene–Sm complex. [d] See Scheme 1 for description of the azacyclic products. [e] The TS structures for 6-*endo* cyclisation by means of a *Si*-diene-face approach could not be located, as they are indicated to be highly unfavourable energetically.

Protonolysis of azacyclic intermediates: As the 6-*endo* cyclisation has been shown before to be effectively precluded kinetically, intermediate **5** does not occur in any appreciable concentration. Accordingly, the path towards piperidine **P7** remains entirely closed, irrespective of whether protonation of **5** is feasible or not. Hence, protonolysis of **4** will be exclusively considered, with the focus on the kinetically most accessible proton transfer onto the terminal C^8 atom of the *syn*-butenyl group,[8b] which gives rise to **6a** and **P6a** on a direct path. This pathway is structurally characterised in Figure 2, whilst the energetics are summarised in Table 3.

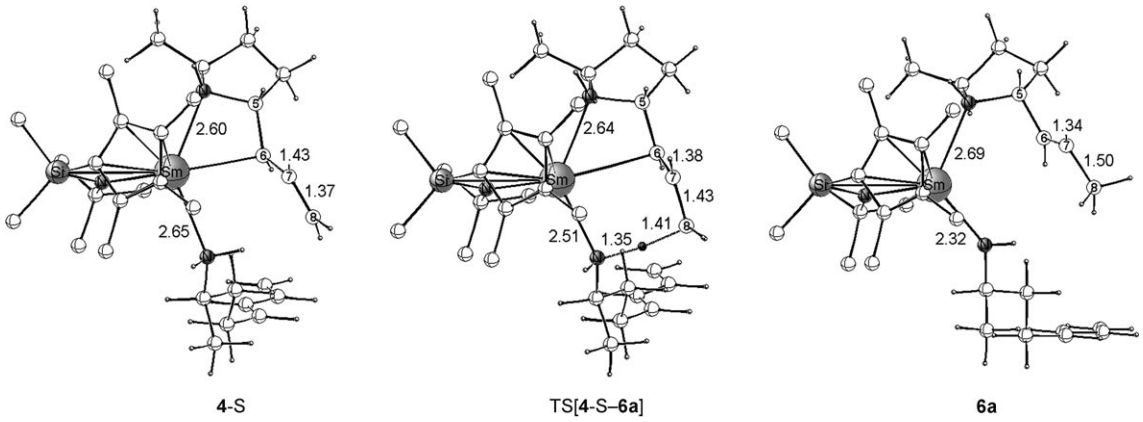

Figure 2. Selected structural parameters [Å] of the optimised structures of key species for protonolysis of the *syn*-η^3-butenyl–Sm intermediate **4** by **1** to afford the cycloamine–amido–Sm complex **6a**. The cut-off for drawing Sm–C bonds was arbitrarily set to 3.1 Å. The hydrogen atoms on the CGC backbone are omitted for the sake of clarity.

Table 3. Energy profile for protonolysis of the *syn*-η^3-butenyl–azacycle–Sm intermediate **4** by aminodiene substrate **1** to afford the cycloamine–amido–Sm compound **6a** along the most accessible pathway for proton transfer onto the terminal butenyl-C^8 centre.[a,b]

Cyclisation pathway	**4**-S	TS	**6a**
5-*exo*			
2,5-*cis* (*Re*)	−0.9/*6.0*	7.1/*14.6*	−7.9/*−2.4*
2,5-*cis* (*Si*)	2.2/*9.1*	9.0/*16.7*	−8.0/*−2.3*
2,5-*trans* (*Re*)	−4.2/*2.5*	5.2/*12.6*	−11.6/*−6.2*
2,5-*trans* (*Si*)	−2.3/*4.4*	3.8/*11.2*	−10.5/*−4.9*

[a] Total barriers and reaction energies are relative to {**4**+**1**}. [b] Activation enthalpies and free energies ($\Delta H^{\neq}/\Delta G^{\neq}$) and reaction enthalpies and free energies ($\Delta H/\Delta G$) are given in kilocalories per mole; numbers in italic type are the Gibbs free energies.

Additional substrate does not appear to accelerate the protonolysis kinetically, thereby confirming our previous findings.[8b] In an analogues fashion to what has been found for the initial precatalyst transformation (see the previous section on precatalyst activation), protonolysis of **4** proceeds first with formation of adduct **4**-S. Incoming substrate has to compete for coordination with the azacycle which is attached to Sm by its nitrogen lone pair and also with the η^3-butenyl–Sm group. As revealed from Figure 2, substrate association comes at the expense of the butenyl–Sm ligation; its mode switches from η^3 to η^1 together with a closer approaching azacycle moiety. Substrate uptake is slightly exothermic by $-4.2\,kcal\,mol^{-1}$ (ΔH, Table 3). The transfer of the proton from associated **1** to the terminal butenyl-C^8 centre evolves through a transition-state structure that constitutes the concomitant N–H bond cleavage and C–H bond formation. This goes along with a butenyl→vinyl conversion of the azacycle's tether, which is partially achieved in TS[**4**-S–**6a**] (Figure 2). This path is connected with a free-energy barrier of $11.2\,kcal\,mol^{-1}$ and leads to **6a** in an exergonic process that is driven by a thermodynamic force of $-6.2\,kcal\,mol^{-1}$. Expulsion of the major pyrrolidine product through **6a**+**1**→**3**-S+**P6a** is a supposedly facile,[25,29] exergonic step ($\Delta G = -2.7\,kcal\,mol^{-1}$), which drives the overall protonolysis step further downhill.

Free-energy profile: The condensed Gibbs free-energy profile, considering only the favourable stereochemical pathways for each of the relevant steps of the catalytic cycle (Scheme 1) is displayed in Figure 3. This gives rise to the following mechanistic conclusions, which are similar to those from our previous study;[8b] thus being briefly summarised: 1) The substrate-adduct **3**-S of the CGC–Sm–amidodiene complex is the thermodynamically prevalent species, thus being the most likely candidate to represent the catalyst's resting state. This is consistent with experimental observation.[3b,4b,7] However, the substrate free form **3′** with a chelating amidodiene group is the direct precursor for ring closure. 2) Intramolecular C–N bond formation and protonolysis are indicated to not be assisted by additive substrate molecules. Accordingly, the substrate must first dissociate from the resting state prior to ring closure. 3) Ring closure proceeds with almost complete regioselectivity through the *exo*-cyclic **3′**→**4** pathway, which gives rise to the five-membered CGC–Sm–azacycle intermediate **4** in a facile ($\Delta G^{\neq} = 5.5\,kcal\,mol^{-1}$) and slightly exergonic transformation. 4) Subsequent protonation of the azacycle's allylic tether of **4** has the highest kinetic barrier of all relevant steps. This turnover-limiting protonolysis is followed by an almost instantaneous **6a**+**1**→**3**-S+**P6a** release of the pyrrolidine product, which drives the overall step further downhill.

Elucidation of the diastereoselectivity: In the second part of this study, the ring substituent diastereoselectivity of the aminodiene IHC is elucidated. As revealed from Figure 3, protonolysis is turnover limiting, whilst the diastereoselectivity is dictated by **3′**→**4** ring closure.[30,31] To analyse the diastereoselectivity of the cyclisation process, a total of four assembly modes must be considered; those are depicted schematically in Scheme 4 for the favourable frontal cyclisation trajectory (cf. the previous section on intramolecular cyclisa-

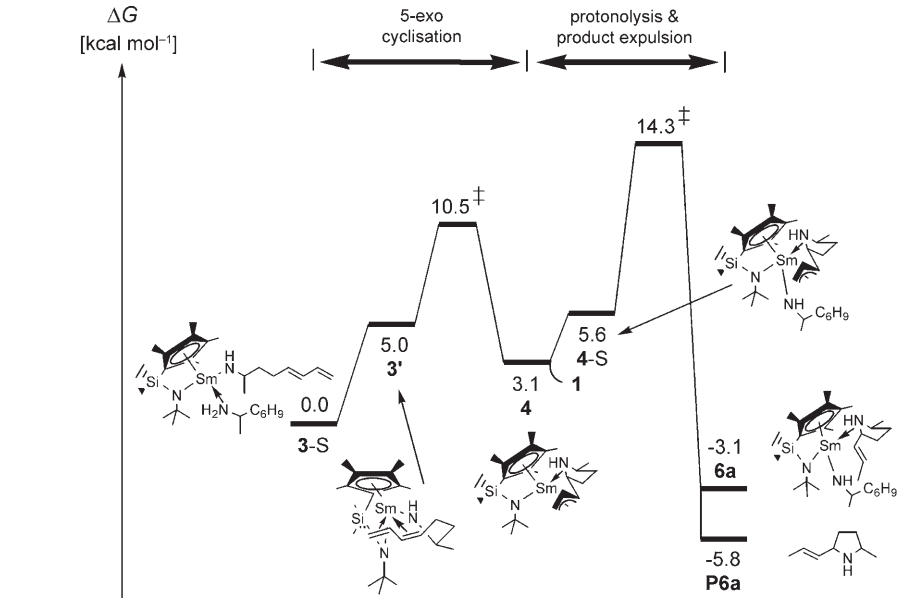

Figure 3. Condensed Gibbs free-energy profile [kcal mol^{-1}] of the intramolecular hydroamination/cyclisation of 1-methyl-(4*E*,6)-heptadienylamine (**1**) mediated by the [(CGC)Sm{N(TMS)$_2$}] precatalyst (**2**). Only the most feasible of the various stereochemical pathways for relevant steps are included. Cycloamine product expulsion through **6a**+**1**→**3**-S+**P6a** is included.

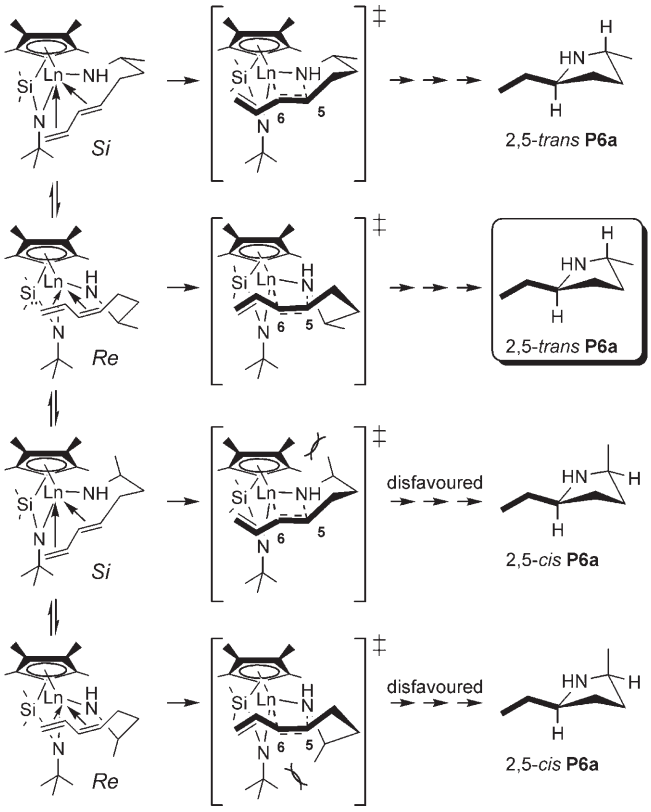

Scheme 4. Stereochemical pathways for diastereoselective intramolecular hydroamination/cyclisation of α-substituted aminodiene **1** by CGC–Ln catalysts to afford disubstituted pyrrolidines by means of a frontal approach of the diene functionality.

tion). The *Re* and *Si* faces of the diene moiety can approach the Ln–N bond, with the α-methyl substituent occupying an equatorial or axial position in the chairlike transition state, thereby giving rise to 2,5-*trans* and 2,6-*cis* pyrrolidine **P6a**, respectively.

Factors governing the ring-substituent diastereoselectivity: Table 2 contains the energetics of the various stereochemical pathways for *exo*cyclic ring closure. The orientation of the α-methyl substituent in the chairlike TS[**3′**–**4**] determines the stereoselectivity. The equatorial methyl group causes minimal interactions with the Cp ring and N*t*Bu group, respectively, with ring closure involving *Re* and *Si* diene faces predicted to be almost degenerate kinetically. The rather small effect of the equatorial α-methyl substituent is seen from the comparison with the achiral (4*E*,6)-heptadienylamine (**1′**). The energy profile for this less encumbered substrate ($\Delta H^{\neq}=4.6$ kcal mol^{-1}, $\Delta G=-1.1$ kcal mol^{-1}, Table S1 in the Supporting Information) is almost identical to the one obtained for *trans*-2,5 pathways (Table 2). In contrast, the axial α-methyl substituent exerts substantial steric pressure onto the Cp ring and N*t*Bu group at all stages of the process (Scheme 4), as indicated by the higher energy of the key species participating along the *cis*-2,5 pathway relative to the ones of the *trans*-2,5 pathway. Considering **3′**, the enthalpic disparity amounts to 2.0 kcal mol^{-1} and unsurprisingly increases to 2.6 kcal mol^{-1} in the transition state, when the favourable *trans*-2,5 and *cis*-2,5 generating pathways are compared (Table 2). Notably, the orientation of the axial α-methyl group towards the Cp ring (*cis*-2,5 pathway, *Si* approach) causes unfavourable steric interactions that are more pronounced than the interaction with the N*t*Bu group along the alternative *Re* approach. This may change upon variation of the lanthanide ion size and introducing some extra steric pressure at the CGC-N centre (see below).

Addition of the *Re* face of the diene's C^5=C^6 double bond across the Sm–N bond along the frontal *exo*cyclic trajectory is the most accessible pathway for the generation of 2,5-*trans* and 2,5-*cis*-disubstituted isomers of **4**.[32] Of the alternative exocyclic pathways, the *trans*-2,5-generating pathway is predicted to be predominant. The calculated kinetic gap of 2.6 kcal mol^{-1} ($\Delta\Delta H^{\neq}$) reveals that both pathways are accessible, but with 2,5-*trans* **P6a** being the major product, and is in reasonable agreement with experiment.[33] It can be concluded that steric interactions between the substrate's α-

substituent and the Cp ring and/or N*t*Bu group of the catalyst's backbone dictates the diastereodifferentiation, as summarised in the stereomodel depicted in Scheme 4.[34] Moreover, α-substituents are vital for stereochemical induction. Probing the β-substituted 2-methyl-(4*E*,6)-heptadienylamine **1″** indicates a significant loss of *trans*/*cis* selectivity,[35] as the $\Delta\Delta H^{\ddagger}$ gap diminishes by half to 1.3 kcal mol^{-1} (Table S1 in the Supporting Information), owing to reduced steric demands caused by a β-substituent.

To validate this model further, substrates **1a**–**c**, in which the α-methyl group is replaced by ethyl, *i*Pr and phenyl groups, respectively, have been considered. As revealed from Table S1 in the Supporting Information the stereodifferentiating gap is almost identical for **1** and **1a** (R = Et, $\Delta\Delta H^{\ddagger}$ = 2.5 kcal mol^{-1}), but increases to $\Delta\Delta H^{\ddagger}$ = 3.3 kcal mol^{-1} (**1b**, R = *i*Pr) and to 4.3 kcal mol^{-1} (**1c**, R = Ph) with the more bulky groups. The TS of the *cis*-2,5 pathway is disfavoured by increasing α-substituent interactions with the N*t*Bu group (*Re* approach) and even more so with the Cp-ring (*Si* approach). Thus, sterically demanding α-alkyl-substituted substrates should greatly enhance the *trans*/*cis* selectivity, whilst the highest diastereoselectivity is predicted for aryl-substituted substrates.

Influence of lanthanide ionic radius and steric bulk at the catalyst backbone: To further elaborate on the sensitivity of ring closure to steric demands, two directions have been pursued. Stereodifferentiation tunability has been investigated, firstly, by variation of metal ionic radius and, secondly, by increasing steric bulk at the catalyst backbone. Considering the former aspect first, Table 4 summarises the energy profile for exocyclic ring closure of **1** by various CGC–Ln (Ln = La, Y, Lu) catalysts.[36] Although CGC–Ln ligation is sterically open, Table 4 shows that variation of the metal's ionic radius has a noticeable influence on *trans*/*cis* selectivity. Our study predicts that the kinetic gap increases regularly upon reduction of the metal's size in the following order, starting from the least congested La system ($\Delta\Delta H^{\ddagger}$ = 2.3 kcal mol^{-1}), Sm ($\Delta\Delta H^{\ddagger}$ = 2.6 kcal mol^{-1}), Y ($\Delta\Delta H^{\ddagger}$ = 3.6 kcal mol^{-1}) and Lu ($\Delta\Delta H^{\ddagger}$ = 4.1 kcal mol^{-1}). As the gap nearly doubles for Lu relative to La, small radius lanthanide catalysts, such as CGC–Lu, might exhibit improved diastereoselectivities. This again originates primarily from greater N*t*Bu/Cp–substrate axial-substituent interactions along the *cis*-2,5 pathway, which are caused by closer interatomic contacts for these sterically more encumbered systems. Unsurprisingly, the frontal trajectory is still the most accessible route for ring closure that is almost exclusively followed. Although of the detailed studies on CGC–Ln catalysts by Marks' group,[7] the effect of the lanthanide ionic radius on *trans*/*cis* selectivity in aminodiene IHC has not been reported thus far. However, a moderate increase in diastereoselectivity for small-radius lanthanide centres has been observed for aminoalkene substrates.[5b,6c]

The effect of increased steric bulk has been further studied for the modified GCG–Ln–amidodiene compounds **3N′**, in which the *t*BuN group is replaced by its silicon analogue. The results are collected in Table S2 in the Supporting Information.

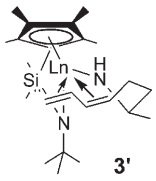

3′

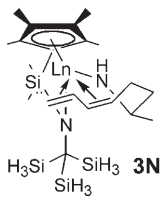

3N′

Table 4. Energy profile for ring closure in the CGC–Ln–amidodiene compound through the exocyclic pathway.[a,b]

Cyclisation pathway	Precursor[c]	TS	$\Delta\Delta H^{\ddagger}$[d]	Product
Ln = La	5.1/*4.2* (**3**)			
2,5-*cis* (*Re*)	2.7/*2.9* (**3′**)	6.1/*7.5*	2.3	−2.6/*−0.8* (**4**)
2,5-*cis* (*Si*)	2.7/*2.9* (**3′**)	7.9/*9.6*	4.1	−0.4/*1.6* (**4**)
2,5-*trans* (*Re*)	0.1/*0.1* (**3′**)	3.8/*5.1*	0.0	−4.2/*−2.3* (**4**)
2,5-*trans* (*Si*)	0.0/*0.0* (**3′**)	4.7/*5.9*	0.9	−3.3/*−1.6* (**4**)
Ln = Y	7.1/*6.2* (**3**)			
2,5-*cis* (*Re*)	3.8/*4.0* (**3′**)	8.3/*9.8*	3.6	−0.8/*1.1* (**4**)
2,5-*cis* (*Si*)	4.1/*4.3* (**3′**)	9.5/*11.2*	4.8	2.0/*4.0* (**4**)
2,5-*trans* (*Re*)	0.6/*0.6* (**3′**)	5.3/*6.6*	0.6	−2.5/*−0.7* (**4**)
2,5-*trans* (*Si*)	0.0/*0.0* (**3′**)	4.7/*6.0*	0.0	−2.5/*−0.8* (**4**)
Ln = Lu	7.5/*6.6* (**3**)			
2,5-*cis* (*Re*)	4.1/*4.3* (**3′**)	8.8/*10.3*	4.1	0.4/*2.2* (**4**)
2,5-*cis* (*Si*)	4.3/*4.5* (**3′**)	9.8/*11.5*	5.1	3.2/*5.2* (**4**)
2,5-*trans* (*Re*)	0.8/*0.8* (**3′**)	5.5/*6.8*	0.8	−1.5/*0.3* (**4**)
2,5-*trans* (*Si*)	0.0/*0.0* (**3′**)	4.7/*6.0*	0.0	−1.9/*−0.2* (**4**)

[a] Total barriers and reaction energies are relative to the favourable isomer **3′** of the substrate-free form of the amidodiene–Ln complex, which has a chelated amidodiene functionality. [b] Activation enthalpies and free energies ($\Delta H^{\ddagger}/\Delta G^{\ddagger}$) and reaction enthalpies and free energies ($\Delta H/\Delta G$) are given in kilocalories per mole; numbers in italic type are the Gibbs free energies. [c] See the text (or Scheme 1) for a description of the various forms of the amidodiene–Ln complex. [d] Relative stability of diastereoisomeric transition states.

The increase of the steric pressure around the CGC N centre does not only influence the directly affected *Re* approach (N–C(SiH$_3$)$_3$–α-substituent contacts, cf. Scheme 4), but also the *Si* pathways, due to some cooperative effects. Of the various pathways, however, disfavouring of the *cis*-2,5 TS (*Re* face) is most pronounced. This gives rise to a noticeable amplification of the kinetic separation between *trans*-2,5 and *cis*-2,5 pathways upon going from **3′** ($\Delta\Delta H^{\ddagger}$ = 2.6 kcal mol^{-1} for Ln = Sm) to **3N′** ($\Delta\Delta H^{\ddagger}$ = 4.0 kcal mol^{-1} for Ln = Sm). The combination of increased bulk at the CGC N centre together with small radius lanthanides greatly in-

fluences the gap to increase, again regularly, to 5.4 and 6.0 kcal mol^{-1} for **3N′** with Ln = Lu, Y (Table S2 in the Supporting Information); thus almost complete *trans* selectivity should be achieved for these catalysts.[37]

Overall, our studies have shown that the ring substituent diastereoselectivity of ring closure can be modulated considerably by varying the lanthanide size and by introducing steric demands at the aminodiene's α-position and/or the CGC N centre. This is likely to affect the reaction rate as well,[38] as observed experimentally.[7]

Conclusion

Presented herein is the computational exploration of intramolecular hydroamination/cyclisation of α-substituted aminodienes in the presence of the constrained geometry [(CGC)Ln{N(TMS)$_2$}] precatalyts. The first survey of relevant elementary steps for the parent substrate **1** and [(CGC)Sm{N(TMS)$_2$}] precatalyst (**2**) revealed the following mechanistic aspects (see also reference [8b]): The substrate-adduct **3**-S of the CGC–Ln–amidodiene complex represents the catalyst's resting state, but the substrate-free form, **3′**, with a chelating amidodiene functionality is the direct precursor for cyclisation. This step proceeds with almost complete regioselectivity through exocyclic ring closure by means of the frontal trajectory, giving rise to the five-membered CGC–Ln–azacycle intermediate **4**. Subsequent protonolysis of **4** has the highest barrier of all relevant steps. Accordingly, protonolysis is turnover limiting, whilst the ring-substituent diastereoselectivity is dictated by exocyclic ring closure.

The present study has elucidated the origin of the diastereoselectivity and has demonstrated the pivotal role of the substrate's α-substituent for stereochemical induction. The *trans*/*cis* selectivity has been rationalised in terms of the stereochemical model depicted in Scheme 4,[34] and the responsible factors have been quantified. Studying of substrates with more bulky α-substituents has validated this model further. As unfavourable interactions between the substrate's α-substituent and the catalyst's backbone are largely dictating the diastereodifferentiation, the variation of the lanthanide's ionic radius and introducing steric pressure at the substrate's α-position and/or CGC N centre have been identified as effective handles for tuning the diastereoselectivity. The quantification of these factors reported herein represents the first step toward the rational design of improved CGC–Ln catalyst architectures and will thus aid this process.

Computational Methods

All DFT calculations were performed with the program package TURBOMOLE[12] by using the TPSS density functional[13] within the RI-*J* approximation[14] in conjunction with flexible basis sets of triple-ζ quality. For Sm, we used the Stuttgart–Dresden quasirelativistic effective core potential (SDD) with the associate (7s6p5d)/[5s4p3d] valence basis set contracted according to a (31111/3111/311/1) scheme.[15] This ECP treats [Kr]4d^{10}4f^5 as a fixed core, whereas 5s^{2}5p^{6}6s^{2}5d^{1}6p^0 shells are taken into account explicitly. All other elements were represented by Ahlrich's valence triple-ζ TZVP basis set[16] with polarization functions on all atoms. The good to excellent performance of the TPSS functional for a wide range of applications has been demonstrated previously.[17] The growing string method[18] was employed for exploring reaction paths, in which two string fragments (commencing from the reactant and product side, respectively) are grown until the two fragments join. As this was performed in mass-weighted coordinates, an approximate to the minimum-energy path (MEP) was obtained. This identified the reactant and product states to be linked to the associated transition state. The approximate saddle point connected with the MEP was subjected to an exact localisation of the TS structure. All stationary points were located by utilizing analytical/numerical gradients/Hessians according to standard algorithms and were identified exactly by the curvature of the potential-energy surface at these points corresponding to the eigenvalues of the Hessian. The gas-phase reaction and activation enthalpies and free energies (ΔH, ΔH^{+} and ΔG, ΔG^{+} at 298 K and 1.0 atm) were evaluated according to standard textbook procedures[19] by using computed harmonic frequencies. Enthalpies were reported as ΔE + zero-point energy corrections at 0 K + thermal motion corrections at 298 K. Gibbs free-energies were obtained as $\Delta G = \Delta H^{+} T\Delta S$ at 298 K. The influence of the solvent was taken into explicit consideration by making use of a continuum model. The experimentally used benzene solvent[7] was described as a homogeneous, isotropic dielectric medium (characterised by its relative static dielectric permittivity $\varepsilon = 2.247$ at 298 K)[20] within the conductor-like screening model (COSMO) due to Klamt and Schüürmann[21] as implemented in TURBOMOLE.[22] Nonelectrostatic contributions to solvation were not included. The solvation effects were included self-consistently, and all the key species were fully located with inclusion of solvation. The solvation enthalpy was approximated by the difference between the electronic energy computed by using the COSMO solvation model and the gas-phase energy. The entropy contributions for condensed-phase conditions were estimated on the basis of the computed gas-phase entropies by employing the procedure of Wertz.[23] Further details of the computational methodology employed are given in the Supporting Information. The mechanistic conclusions drawn in this study were based on the computed Gibbs free-energy profile of the overall reaction for experimental condensed-phase conditions (Scheme 1). Enthalpies were referred to in the elucidation of the diastereoselectivity control, as entropy contributions are almost identical for alternative stereochemical pathways. All the drawings were prepared by employing the StrukEd program.[24]

[1] For reviews of catalytic hydroamination see: a) L. S. Hegedus, *Angew. Chem.* **1988**, *100*, 1147; *Angew. Chem. Int. Ed.* **1998**, *27*, 1113; b) D. M. Roundhill, *Catal. Today* **1997**, *37*, 155; c) T. E. Müller, M. Beller, *Chem. Rev.* **1998**, *98*, 675; d) M. Nobis, B. Drießen-Hölscher, *Angew. Chem.* **2001**, *113*, 4105; *Angew. Chem. Int. Ed.* **2001**, *40*, 3983; e) R. Taube in *Applied Homogeneous Catalysis with Organometallic Complexes* (Eds.: B. Cornils, W. A. Herrmann), Wiley-VCH, Weinheim, **2002**, pp. 513–524; f) J. Seayad, A. Tillack, C. G. Hartung, M. Beller, *Adv. Synth. Catal.* **2002**, *344*, 795; g) F. Pohlki, S. Doye, *Chem. Soc. Rev.* **2003**, *32*, 104; h) P. W. Roesky, T. E. Müller, *Angew. Chem.* **2003**, *115*, 2812; *Angew. Chem. Int. Ed.* **2003**, *42*, 2708; i) J. F. Hartwig, *Pure Appl. Chem.* **2004**, *76*, 507; j) K. C. Hultzsch, *Adv. Synth. Catal.* **2005**, *347*, 367.

[2] a) T. J. Marks, R. D. Ernst, in *Comprehensive Organometallic Chemistry* (Eds.: G. Wilkinson, F. G. A. Stone, E. W. Abel), Pergamon Press, Oxford, **1982**, Chapter 21; b) W. J. Evans, *Adv. Organomet. Chem.* **1985**, *24*, 131; c) C. J. Schaverien, *Adv. Organomet. Chem.* **1994**, *36*, 283; d) H. Schumann, J. A. Meese-Marktscheffel, L. Esser, *Chem. Rev.* **1995**, *95*, 865; e) F. T. Edelmann, in *Comprehensive Organometallic Chemistry* (Eds.: G. Wilkinson, F. G. A. Stone, E. W. Abel), Pergamon Press, Oxford, **1995**, Chapter 2; f) R. Anwander, W. A. Herrmann, *Top. Curr. Chem.* **1996**, *179*, 1; g) F. T. Edelmann, *Curr. Chem.* **1996**, *179*, 247; h) *Topics in Organometallic*

Chemistry, Vol. 2 (Ed.: S. Kobayashi), Springer, Berlin, **1999**; i) M. N. Bochkarev, *Chem. Rev.* **2002**, *102*, 2089; j) S. Arndt, J. Okuda, *Chem. Rev.* **2002**, *102*, 1953; k) F. T. Edelmann, D. M. M. Freckmann, H. Schumann, *Chem. Rev.* **2002**, *102*, 1851; l) H. C. Aspinall, *Chem. Rev.* **2002**, *102*, 1807.

[3] For cyclohydroamination mediated by organolanthanides see: a) M. R. Gagné, T. J. Marks, *J. Am. Chem. Soc.* **1989**, *111*, 4108; b) M. R. Gagné, T. J. Marks, *J. Am. Chem. Soc.* **1992**, *114*, 275; c) Y. Li, P.-F. Fu, T. J. Marks, *Organometallics* **1994**, *13*, 439; d) Y. Li, T. J. Marks, *J. Am. Chem. Soc.* **1996**, *118*, 9295; e) G. A. Molander, E. D. Dowdy, *J. Org. Chem.* **1998**, *63*, 8983; f) M. R. Bürgstein, H. Berberich, P. W. Roesky, *Organometallics* **1998**, *17*, 1452; g) A. T. Gilbert, B. L. Davis, T. J. Emge, R. D. Broene, *Organometallics* **1999**, *18*, 2125; h) G. A. Molander, E. D. Dowdy, *J. Org. Chem.* **1999**, *64*, 6515; i) Y. K. Kim, T. Livinghouse, J. E. Bercaw, *Tetrahedron Lett.* **2001**, *42*, 2944; j) G. A. Molander, E. D. Dowdy, S. K. Pack, *J. Org. Chem.* **2001**, *66*, 4344; k) M. R. Bürgstein, H. Berberich, P. W. Roesky, *Chem. Eur. J.* **2001**, *7*, 7078; l) S. Hong, T. J. Marks, *J. Am. Chem. Soc.* **2002**, *124*, 7886; m) S. Hong, S. Tian, M. V. Metz, T. J. Marks, *J. Am. Chem. Soc.* **2003**, *125*, 14768; n) A. Zulys, T. K. Panda, M. T. Gamer, P. W. Roesky, *Chem. Commun.* **2004**, 2584.

[4] a) G. A. Molander, J. A. C. Romero, *Chem. Rev.* **2002**, *102*, 2161; b) S. Hong, T. J. Marks, *Acc. Chem. Res.* **2004**, *37*, 673.

[5] a) P. J. Shapiro, M. D. Cotter, W. P. Schaefer, J. A. Labinger, J. E. Bercaw, *J. Am. Chem. Soc.* **1994**, *116*, 4623; b) S. Tian, V. A. Arredondo, C. L. Stern, T. J. Marks, *Organometallics* **1999**, *18*, 2568; c) K. C. Hultzsch, T. P. Spaniol, J. Okuda, *Angew. Chem.* **1999**, *111*, 178; *Angew. Chem. Int. Ed.* **1999**, *38*, 227; d) S. Arndt, J. Okuda, *Chem. Rev.* **2002**, *102*, 953; e) J. Okuda, *Dalton Trans.* **2003**, 2367; f) B. D. Stubbert, C. L. Stern, T. J. Marks, *Organometallics* **2003**, *22*, 4836.

[6] a) V. M. Arredondo, S. Tian, F. E. McDonald, T. J. Marks, *J. Am. Chem. Soc.* **1999**, *121*, 3633; b) J.-S. Ryu, T. J. Marks, F. E. McDonald, *Org. Lett.* **2001**, *3*, 3091; c) J.-S. Ryu, T. J. Marks, F. E. McDonald, *J. Org. Chem.* **2004**, *69*, 1038; d) A. M. Seyam, B. D. Stubbert, T. R. Jensen, J. J. O'Donnell, III, C. S. Stern, T. J. Marks, *Inorg. Chim. Acta* **2004**, *357*, 4029.

[7] a) S. Hong, T. J. Marks, *J. Am. Chem. Soc.* **2002**, *124*, 7886; b) S. Hong, A. M. Kawaoka, T. J. Marks, *J. Am. Chem. Soc.* **2003**, *125*, 15878.

[8] For computational studies of organolanthanide-assisted intramolecular hydroamination/cyclisation of various substrate classes see: aminoalkene substrates a) A. Motta, G. Lanza, I. L. Fragala, T. J. Marks, *Organometallics* **2004**, *23*, 4097; aminodiene substrates b) S. Tobisch, *J. Am. Chem. Soc.* **2005**, *127*, 11979; aminoallene substrates c) S. Tobisch, *Chem. Eur. J.* **2006**, *12*, 2520; aminoalkyne substrates d) A. Motta, I. L. Fragala, T. J. Marks, *Organometallics* **2006**, *25*, 5533.

[9] The mechanism proposed by Marks for organolanthanide-mediated IHC (reference 4b) has been shown to be operational for cationic Group 4 metal catalysts as well see: a) S. Tobisch, *Dalton Trans.* **2006**, 4277. The IHC catalysed by neutral Group 4 metal compounds, however, follows a different mechanism see: b) S. Tobisch, *Chem. Eur. J.* **2007**, *13*, 4884.

[10] Scheme 1 comprises exclusively of the alternative 5-*exo* and 6-*endo* cyclisation paths, which dictate the regioselectivity of ring closure, and the most accessible of the various pathways for protonolysis of intermediate **4** that leads directly to the predominant cycloamine **P6a**. The protonolysis path toward **P7** is included for completeness only, although it is entirely suppressed by both kinetic and thermodynamic factors. Please see reference [8b] for a detailed computational scrutinisation of an almost complete set of alternative pathways for relevant steps in aminodiene IHC.

[11] Other possible pyrrolidines are 2-methyl-5-[(*Z*)-prop-1-enyl]pyrrolidine (**P6b**), to be formed by protonation of the terminal C^8-allylic centre of the *anti*-η^3-butenyl–Ln isomer of **4**, and 2-methyl-5-(prop-2-enyl)pyrrolidine (**P6c**), to be generated by protonation of the substituted C^6-allylic centre of either *syn*- or *anti*-η^3-butenyl–Ln isomers of **4**, respectively. Please see reference [8b] for more details.

[12] a) R. Ahlrichs, M. Bär, M. Häser, H. Horn, C. Kölmel, *Chem. Phys. Lett.* **1989**, *162*, 165; b) O. Treutler, R. Ahlrichs, *J. Chem. Phys.* **1995**, *102*, 346.

[13] a) P. A. M. Dirac, *Proc. R. Soc. London Ser. A Proc. R. Soc. London Ser. B* **1929**, *A123*, 714; b) J. C. Slater, *Phys. Rev.* **1951**, *81*, 385; c) J. P. Perdew, Y. Wang, *Phys. Rev.* **1992**, *B45*, 13244; d) J. Tao, J. P. Perdew, V. N. Staroverov, G. E. Scuseria, *Phys. Rev. Lett.* **2003**, *91*, 146401; e) J. P. Perdew, J. Tao, V. N. Staroverov, G. E. Scuseria, *J. Chem. Phys.* **2004**, *120*, 6898.

[14] a) O. Vahtras, J. Almlöf, M. W. Feyereisen, *Chem. Phys. Lett.* **1993**, *213*, 514; b) K. Eichkorn, O. Treutler, H. Öhm, M. Häser, R. Ahlrichs, *Chem. Phys. Lett.* **1995**, *242*, 652.

[15] M. Dolg, H. Stoll, A. Savin, H. Preuß, *Theor. Chim. Acta* **1989**, *75*, 173.

[16] A. Schäfer, C. Huber, R. Ahlrichs, *J. Chem. Phys.* **1994**, *100*, 5829.

[17] a) V. N. Staroverov, G. E. Scuseria, J. Tao, J. P. Perdew, *J. Chem. Phys.* **2003**, *119*, 12129; b) Y. Zao, D. G. Truhlar, *J. Chem. Theory Comput.* **2005**, *1*, 415; c) F. Furche, J. P. Perdew, *J. Chem. Phys.* **2006**, *124*, 044103.

[18] a) B. Peters, A. Heyden, A. T. Bell, A. Chakraborty, *J. Chem. Phys.* **2004**, *120*, 7877; b) A. Heyden, personal communication, **2007**.

[19] D. A. McQuarrie, Statistical Thermodynamics, Harper & Row, New York, 1973.

[20] CRC Handbook of Chemistry and Physics, 84th ed. (Ed.: D. R. Lide), CRC Press, New York, **2003–2004**.

[21] a) A. Klamt, G. Schüürmann, *J. Chem. Soc. Perkin Trans. 2* **1993**, 799; b) A. Klamt in *Encyclopedia of Computational Chemistry, Vol. 1* (Ed.: P. von R. Schleyer), Wiley, Chichester, **1998**, pp. 604–615.

[22] A. Schäfer, A. Klamt, D. Sattel, J. C. W. Lohrenz and F. Eckert, *Phys. Chem. Chem. Phys.* **2000**, *2*, 2187.

[23] D. H. Wertz, *J. Am. Chem. Soc.* **1980**, *102*, 5316.

[24] For further details, see http://www.struked.de.

[25] Examination by a linear-transit approach gave no indication that this process is associated with a significant enthalpic barrier.

[26] Precursor **3′** readily complexes **1** to form a stable adduct **3**-S. However, transition-states TS[**3′–4**] and TS[**3′–5**] do not benefit from substrate association, as the located TS[**3′–4**]-S and TS[**3′–5**]-S are uphill in free energy.

[27] a) M. R. Gagné, L. Brard, V. P. Conticello, M. A. Giardello, C. L. Stern, T. J. Marks, *Organometallics* **1992**, *11*, 2003; b) M. A. Giadello, V. P. Conticello, L. Brard, M. Sabat, A. L. Rheingold, C. L. Stern, T. J. Marks, J. Am. Chem. Soc. 1994, 116, 10212; c) M. R. Douglass, M. Ogasawara, S. Hong, M. V. Metz, T. J. Marks, *Organometallics* **2002**, *21*, 283.

[28] See: M. B. Smith, J. March, *March's Advanced Organic Chemistry*, 6th ed., Wiley, New York, **2007**, pp. 305–307.

[29] For NMR spectroscopic evidence of rapid amido/amine permutation and association of free amine see reference [3b].

[30] All the precursor species **3′** of the stereochemical pathways depicted in Figure 3—to be generated through **6a+1**→**P6a+3**-S→**3′+1** product release—have a comparable probability of occurrence, such that the likelihood to enter a pathway is discriminated kinetically by the disparity in enthalpy of the corresponding TS[**3′–4**].

[31] Although the **3′**→**4** ring closure is predicted to be almost thermoneutral, the stereo information is saved after passing through a stereochemical pathway, as the different stereoisomers of **3′** are not likely to be interconvertible on the time scale of cyclisation (and subsequent protonolysis); this would require some **3′**⇔**3**⇔**3′** conversions together with rearrangements in the amidodiene moiety.

[32] These CGC–Sm–azacycle species, furthermore, represent the direct precursor for the most viable pathways for turnover-limiting protonolysis, leading directly to 2,5-*trans* and 2,6-*cis*-pyrrolidine **P6a**, respectively.

[33] The calculated $\Delta\Delta H^{+}$ gap of 2.6 kcal mol^{-1} corresponds to diastereoselectivity of 98.8:1.2 (298.15 K) on application of Stefan–Boltzmann statistics. It is in reasonable agreement with the observed diastereoselectivity of 90:10, which transforms into $\Delta\Delta H^{+} = 1.3$ kcal mol^{-1} (298.15 K).

[34] A similar model has been proposed earlier by Marks and co-workers (references [4b,6c,7b]) for cyclohydroamination of aminoalkenes and aminoalkynes by CGC–Ln catalysts.
[35] Please note the inverted *cis*/*trans* selectivity for formation of the 2,4-disubstituted pyrrolidine.
[36] Representative eight-coordinate effective ionic radii: $La^{3+} = 1.160$, $Sm^{3+} = 1.079$, $Y^{3+} = 1.019$, $Lu^{3+} = 0.977$ Å, see: a) R. D. Shannon, *Acta Crystallogr. Sect. A* **1976**, *32*, 751; b) Y. Q. Jia, *J. Solid State Chem.* **1991**, *95*, 184.
[37] The computed $\Delta\Delta H^{\ddagger}$ gap indicates almost complete *trans* selectivity, irrespective of the slight discrepancy between computationally predicted and observed selectivities for the parent CGC–Sm catalyst (reference [33]).
[38] This, however, is outside of the scope of the present study and will be communicated in a forthcoming manuscript.

Received: April 23, 2007
Published online: August 8, 2007

